Rare earth 4f hybridization with the GaN valence band

2012 Semicond. Sci. Technol. 27 115017

(http://iopscience.iop.org/0268-1242/27/11/115017)

Report Documentation Page

Form Approved
OMB No. 0704-0188

1. REPORT DATE	2. REPORT TYPE	3. DATES COVERED
16 OCT 2012		**00-00-2012 to 00-00-2012**

4. TITLE AND SUBTITLE	5a. CONTRACT NUMBER
Rare earth 4f hybridization with the GaN valence band	5b. GRANT NUMBER
	5c. PROGRAM ELEMENT NUMBER
6. AUTHOR(S)	5d. PROJECT NUMBER
	5e. TASK NUMBER
	5f. WORK UNIT NUMBER
7. PERFORMING ORGANIZATION NAME(S) AND ADDRESS(ES) **Air Force Institute of Technology,Department of Engineering Physics, 2950 Hobson Way,Wright Patterson Air Force Base, Dayton,OH,45433**	8. PERFORMING ORGANIZATION REPORT NUMBER
9. SPONSORING/MONITORING AGENCY NAME(S) AND ADDRESS(ES)	10. SPONSOR/MONITOR'S ACRONYM(S)
	11. SPONSOR/MONITOR'S REPORT NUMBER(S)

12. DISTRIBUTION/AVAILABILITY STATEMENT
Approved for public release; distribution unlimited

13. SUPPLEMENTARY NOTES
Semiconductor Science And Technology, 27 (2012), 7 pages

14. ABSTRACT
The placement of the Gd, Er and Yb 4f states within the GaN valence band has been explored by both experiment and theory. The 4d?4f photoemission resonances for various rare-earth(RE)-doped GaN thin films (RE = Gd, Er, Yb) provide an accurate depiction of the occupied 4f state placement within the GaN. The resonant photoemission show that the major Er and Gd RE 4f weight is at about 5?6 eV below the valence band maximum, similar to the 4f weights in the valence band of many other RE-doped semiconductors. For Yb, there is a very little resonant enhancement of the valence band of Yb-doped GaN, consistent with a large 4f14-δ occupancy. The placement of the RE 4f levels is in qualitative agreement with theoretical expectations.

15. SUBJECT TERMS

16. SECURITY CLASSIFICATION OF:			17. LIMITATION OF ABSTRACT	18. NUMBER OF PAGES	19a. NAME OF RESPONSIBLE PERSON
a. REPORT	b. ABSTRACT	c. THIS PAGE			
unclassified	**unclassified**	**unclassified**	**Same as Report (SAR)**	**9**	

Semicond. Sci. Technol. **27** (2012) 115017 (7pp) doi:10.1088/0268-1242/27/11/115017

Rare earth 4f hybridization with the GaN valence band

Lu Wang[1], Wai-Ning Mei[1], S R McHale[2], J W McClory[2], J C Petrosky[2], J Wu[3], R Palai[3], Y B Losovyj[4] and P A Dowben[5,6]

[1] Department of Physics, University of Nebraska at Omaha, Omaha, NE 68182-0266, USA
[2] Department of Engineering Physics, Air Force Institute of Technology, 2950 Hobson Way, Wright Patterson Air Force Base, Dayton, OH 45433, USA
[3] Department of Physics and Institute for Functional Nanomaterials, University of Puerto Rico, San Juan, PR 00931, USA
[4] The J. Bennett Johnston Sr. Center for Advanced Microstructures and Devices, Louisiana State University, 6980 Jefferson Hwy, Baton Rouge, LA 70806, USA
[5] Department of Physics and Astronomy, Nebraska Center for Materials and Nanoscience, Theodore Jorgensen Hall, 855 North 16th Street, University of Nebraska, PO Box 880299, Lincoln, NE 68588-0299, USA

E-mail: pdowben@unl.edu

Received 23 July 2012, in final form 31 August 2012
Published 16 October 2012
Online at stacks.iop.org/SST/27/115017

Abstract
The placement of the Gd, Er and Yb 4f states within the GaN valence band has been explored by both experiment and theory. The 4d–4f photoemission resonances for various rare-earth(RE)-doped GaN thin films (RE = Gd, Er, Yb) provide an accurate depiction of the occupied 4f state placement within the GaN. The resonant photoemission show that the major Er and Gd RE 4f weight is at about 5–6 eV below the valence band maximum, similar to the 4f weights in the valence band of many other RE-doped semiconductors. For Yb, there is a very little resonant enhancement of the valence band of Yb-doped GaN, consistent with a large $4f^{14-\delta}$ occupancy. The placement of the RE 4f levels is in qualitative agreement with theoretical expectations.

(Some figures may appear in colour only in the online journal)

1. Introduction

In recent decades, rare earth (RE)-doped semiconductors have generated interest due to their applications in new optoelectronic devices [1–4]. III-nitride semiconductors, such as AlN, GaN and InN offer tunable band gaps and favorable thermal, chemical and electronic properties, which facilitate various device applications [5–9] from the ultraviolet through the visible and the infrared range. Moreover, thin film electroluminescent phosphors with red, blue, and green emissions [7–14] imply the promise of full color (white) light capability. Rare earth (RE) doping GaN might have a number of advantages. For example, there is the promise that Eu or Er doping of GaN will improve the light output and that the different luminescence colors for the different REs can be utilized. The centers of luminescence in the RE-doped GaN will play a dominant role in the light yield. Luminescence due to the Er intra-4f-shell transition from the $^4I_{13/2}$ excited state to the $^4I_{15/2}$ ground state is known to be particularly intense and above all, efficient. Due to their highly localized 4f electrons [15–16], the direct f–f interaction luminescence of rare-earth impurities in semiconducting host materials is well interpreted in terms of ionic models perturbed by the crystal field of the host [17–18]. What has been less explored is the influence of the semiconductor host on the direct f–f transitions of an RE dopant [19–21]. The hybridization of the 4f states with the host material valence band could be a good indicator of changes in the luminescence of the dopant as a result of the host material.

Luminescence occurs by means of the energy transfer to a self-trapped exciton in the GaN host, followed by radiative decay (annihilation) [22]. The color and luminescence efficiencies of these decays will be affected by placement

[6] Author to whom any correspondence should be addressed.

and hybridization of the RE dopant 4f states within the GaN valence and conduction bands. The carrier lifetimes or the decay times are important in understanding of the role of the dopants, but are clearly not the only factor. While numerous resonant photoemission studies of RE metals have been reported, the resonant processes resulting from photon interaction with III-nitride semiconductors are significantly less well understood. The 4d–4f photoemission resonances for various RE-doped GaN thin films (RE = Gd, Er, Yb) have now been reported [23]. Plucinski *et al* [24] reported a resonant photoemission process at the Ga 3p absorption threshold in GaN and compared the results to those reported for GaP and GaAs [25, 26]. Additionally, Maruyama *et al* [27] reported on Eu:GaN using x-ray photoelectron spectroscopy (XPS) and resonant photoemission spectroscopy (RPES) and concluded, via 4d–4f resonant photoemission measurements, that the transition from trivalent to divalent Eu ions occurred near the surface of GaN. The key value of resonant photoemission, however, is to probe which valence bands of the semiconductor host have strong 4f and/or RE weight [23, 28–30].

2. Experimental details

As previously described, the $RE_xGa_{1-x}N$ thin films (50–300 nm) were fabricated on Si(111) (RE = Yb, Gd) and sapphire, Al_2O_3 (RE = Er) substrates by RF plasma (EPI 620) assisted molecular beam epitaxy (MBE) [23, 31]. The growth parameters for the deposition of RE-doped (*in situ*) GaN thin films were a base pressure of $\sim 10^{-11}$ Torr, nitrogen flux of 0.75–1.0 SCCM (Yb, Gd) and 2.0 SCCM (Er), RF power of 500 W, substrate temperature of 850–900 °C, Ga cell temperature of 850 °C and RE cell temperatures of 500–850 °C (Yb), 1000–1100 °C (Er) and 1050–1100 °C (Gd). The thickness of the films was measured with a surface profilometer and atomic force microscopy.

The orientation, crystal structure and phase purity of the films were established by Cu K_α (λ = 1.5406 Å) radiation x-ray diffraction using a Siemens D5000 x-ray diffractometer. The x-ray diffraction (XRD) pattern of Yb-, Er- and Gd-doped GaN films show *c*-axis orientation and a high degree of crystallinity [23, 31]. The presence of any secondary phases or spurious peaks has not been observed, as described elsewhere [31, 32]. Slight shifts in diffraction peak positions toward lower Bragg angles have been observed with Er-doped GaN grown on Al_2O_3(0 0 0 1) substrates and $RE_xGa_{1-x}N$ thin films (50–300 nm) fabricated on Si(1 1 1) (RE = Yb,Gd), which is indicative of some lattice expansion, as expected [32]. The *c*-axis length of Yb:GaN was found to be 5.172 Å [32], which is very close to the widely reported and accepted *c*-axis length (5.166 Å) of undoped GaN.

The elemental compositions of the RE-doped GaN thin films grown under different conditions were characterized by energy dispersive spectroscopy (EDS) and a VG Microtech x-ray photoemission system attached to the MBE growth system (VG Microtech). The measured concentrations were found to be at 1–2%, as confirmed from the Ga $2p_{3/2}$, Er 4d, Gd 4d, Yb 4d, and N 1s core level XPS intensities using an AlK_α(1486.8 eV) x-ray source. The typical values for Er concentrations were found to be ∼5%, higher than the EDS- and XPS-derived Gd and Yb concentrations. In these RE-doped GaN samples, surface segregation cannot be excluded and may well be likely, at least in the selvedge region of the surface.

The photoemission experiments were conducted on the 3 m TGM beamline [33] at the Center for Advanced Microstructures and Devices at Louisiana State University [34–36]. The beamline is equipped with a photoemission endstation with a 50 mm hemispherical electron energy analyzer, with a resolution of about 70 meV, as described elsewhere [33, 37]. Photoemission spectra were taken with a 45° incidence angle and the photoelectrons collected along the sample normal. All spectra presented are normalized to the photon flux, and the secondary electron background has been subtracted. The position of the Fermi level was established using a clean Ta foil as reference. All binding energies reported here are with respect to this common Fermi level in terms of $E–E_F$, so that occupied state binding energies are negative. Energy distribution curves (EDCs) were obtained by fixing the photon energy $h\nu$ and sweeping electron kinetic energy E_K. Constant initial state spectra were obtained by simultaneously sweeping $h\nu$ and E_K, so as to hold the binding energy fixed.

Atomically clean GaN:RE surfaces were obtained by several preparatory cycles of Ar^+ ion sputtering and annealing, as described elsewhere [23, 31, 32]. This will create a number of point defects, but photoemission is generally insensitive to such defects. The photoemission spectra from the clean sample surface indicated that the surfaces were free of contaminants.

3. Density functional theory studies of GaN-doped with Gd, Er and Yb

Our calculations are carried out within density function theory (DFT) as implemented in the CASTEP code [38]. The plane wave basis set with energy cutoff around 320 eV, ultra-soft pseudopotential are employed together with the generalized gradient approximation (GGA) and Perdew–Burke–Ernzerhof (PBE) exchange and correlation functional [39]. In addition, we utilize the ensemble density functional theory (EDFT) [40, 41] scheme in CASTEP to overcome the convergence problem inherent in the RE system.

The conventional DFT often fails to describe systems with strongly correlated d and f electrons. Here we used DFT+U method for the corrections of on-site Coulomb interactions with the terms of the effective on-site Coulomb and exchange parameters, U and J, which affect the placement of d and f electron states significantly and are often adjusted to reach agreement with experiment in some sense. Here we employed U = 6 eV and J = 0 eV for 4f electrons of Gd, Er, and Yb, consistent with that of U = 6.7 eV and J = 0.7 eV previously determined for gadolinium metal [42, 43], GdX (X = N, P, As, and Bi) [44, 45] and the endofullerene $Gd_3N@C_{80}$ [46], but less than the value of U = 7.0 eV for GdAuMg [47], U = 7.6 eV, J = 0.6 eV for Gd_2O_3 [48] and the endofullerene $Gd@C_{60}$ [49] and far less than the U = 8.6 eV, J = 0.75 eV used for ErAs [50]. The consequence of choosing too small a value for the effective on-site Coulomb parameter, U, will

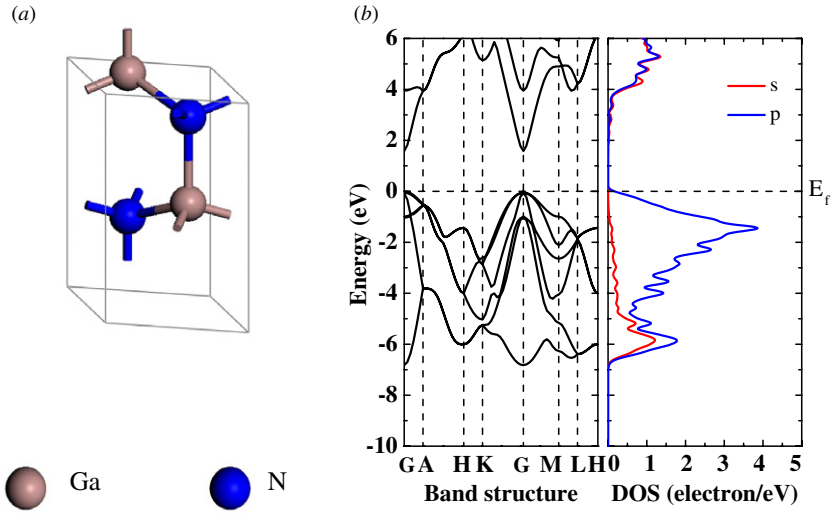

Figure 1. The (*a*) geometric structure, (*b*) band structure and DOS of GdN bulk.

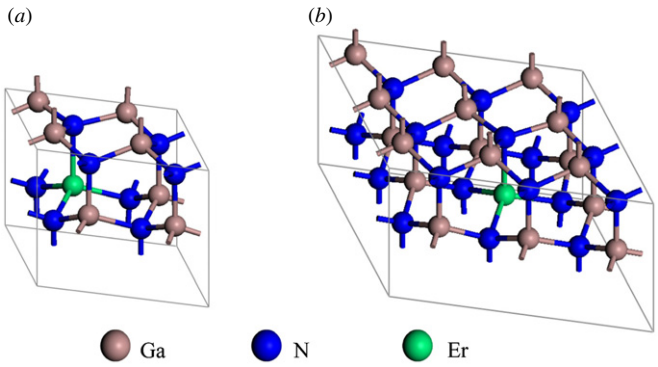

Figure 2. The optimized structure of (*a*) Ga7ErN8, (*b*) Ga17ErN18, as an example to all the rare-earth-doped GaN systems studied.

be that the calculated 4f placements may have far smaller binding energies in theory than observed in the photoemission experiment, although the qualitative placements should be in fact very good indicators of experiment. In fact, the choice of 6 eV as U is the default value for the Hubbard U in the CASTEP code (from La to Yb $U = 6$ eV for f electrons), but variations from experiment abound, as for EuAuMg and YbAuMg, U is seen to be 7 and 0 eV, respectively, for f electrons [47].

We built the hexagonal unit cell of GaN bulk, as showed in figure 1, and then we constructed $2 \times 2 \times 1$ and $3 \times 3 \times 1$ supercells with one Ga atom substituted by Gd, Er, or Yb atom (figure 2), representing 12.5% and 5.5% atomic doping (Ga_7REN_8 and $Ga_{17}REN_{18}$, RE = rare earths), respectively. Monkhorst-Pack [51] $9 \times 9 \times 5, 4 \times 4 \times 5$, and $3 \times 3 \times 5$ k-point grids were adopted for Brilliouin zone sampling of the unit cell of GaN and $2 \times 2 \times 1$ and $3 \times 3 \times 1$ supercells, respectively. Geometry optimizations were performed for the coordinates of the atoms and the lattice parameters until the maximum force on the atoms was less than 0.03 eV/Å and the maximum stress was smaller than 0.05 GPa. Density of states (DOS) of RE 4f levels within the GaN host have been specifically projected out and presented on the side of the band structures as shown in figures 3–5 and in right panels in figures 6–8, to demonstrate their placements and for use in comparison with the photoemission spectra.

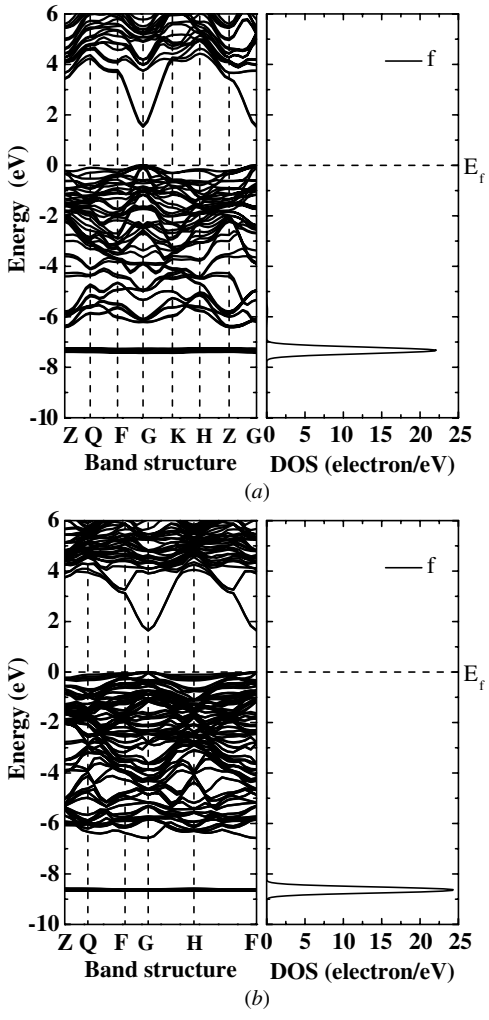

Figure 3. The band structures of the Gd-doped GaN (left), density of states (DOS) of the rare earth Gd 4f weighted contributions within the GaN host (right) for (*a*) Ga_7GdN_{18} and (*b*) $Ga_{17}GdN_{18}$.

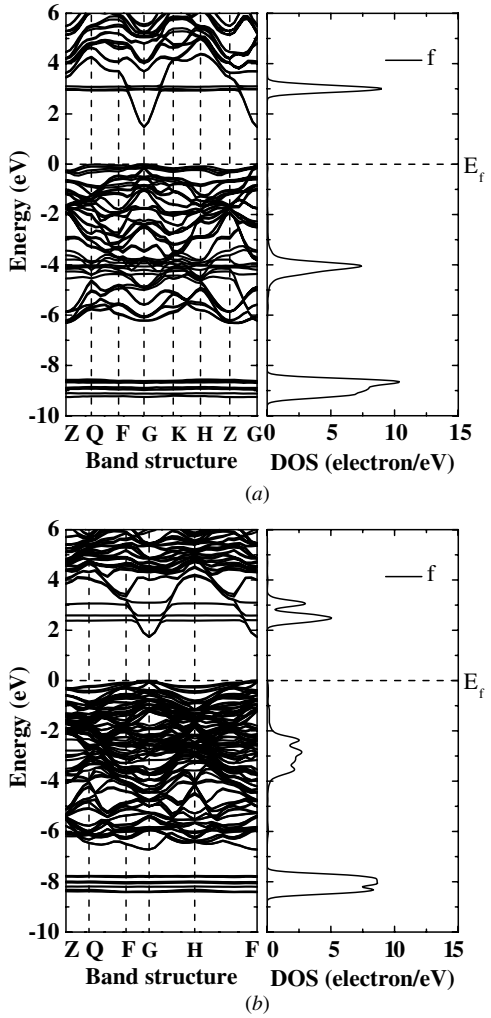

Figure 4. The band structures of the Er-doped GaN (left), DOS of the rare earth Er 4f weighted contributions within the GaN host (right) for (*a*) Ga_7ErN_{18} and (*b*) $Ga_{17}ErN_{18}$.

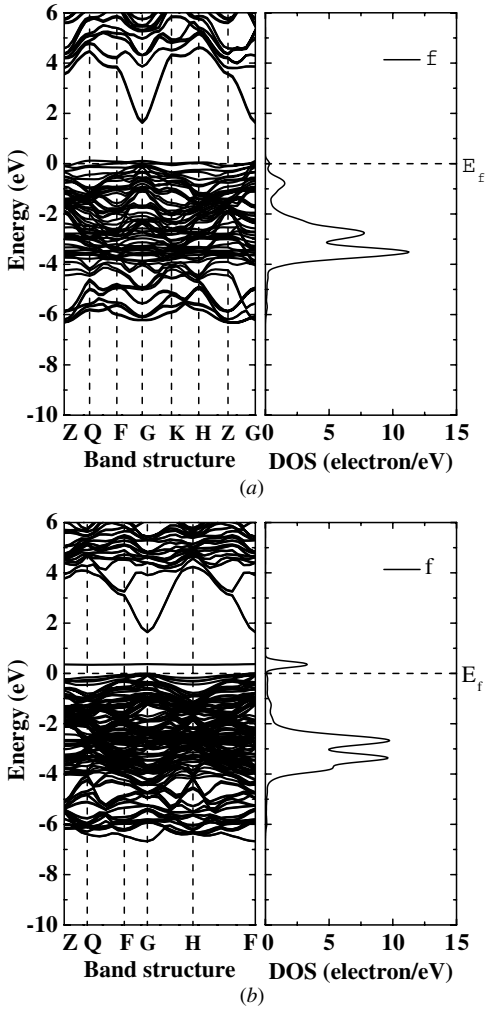

Figure 5. Band structures of the Yb-doped GaN (left), DOS of the rare earth Yb 4f weighted contributions within the GaN host (right) for (*a*) Ga_7YbN_{18} and (*b*) $Ga_{17}YbN_{18}$.

Table 1. Calculated band gaps, supercells, and optimized lattice constants for pristine and doped GaN. Note that all the *a* values of the doped GaN are greater than two or three times that of the pristine, yet the value of *c* only changed slightly.

			Lattice (Å)	
	Band gap (eV)	Supercell	*a*	*c*
GaN	1.58	1 × 1 × 1	3.23	5.27
$Ga7GdN_8$	1.52	2 × 2 × 1	6.62	5.33
$Ga17GdN_{18}$	1.64	3 × 3 × 1	9.79	5.28
$Ga7ErN_8$	1.48	2 × 2 × 1	6.63	5.33
$Ga17ErN_{18}$	1.73	3 × 3 × 1	9.73	5.24
$Ga7YbN_8$	1.50[a]	2 × 2 × 1	6.60	5.31
$Ga17YbN_{18}$	1.29[a]	3 × 3 × 1	9.77	5.27

[a] Counting from the top of the impurity band to the bottom of the conduction band.

We noted that the optimized lattices *a* of the doped GaN with 2 × 2 × 1 or 3 × 3 × 1 supercell, listed in Table 1, are slightly larger than 2 or 3 times that of the undoped pristine GaN, thus bigger strain is expected. For the calculated band structure of GaN bulk, we find it to be a semiconductor. Indeed, all of the RE-doped GaN systems calculated were found to be semiconducting, except Ga_7YbN_8, which we predict to be metallic. The narrow 4f bands generally have very small band dispersion and can be generally identified with the help of 4f DOS in the right panels and in comparison with the band structure of GaN bulk.

4. Identification of the 4f contributions to the valence band of doped GaN

Resonant photoemission is a premier tool for identifying the occupied 4f positions of REs in the photoemission spectra of a semiconductor host [23, 27–30, 48]. Figures 6–8 (doping with Gd, Er and Yb, respectively) show the valence band photoemission spectra at various photon energies in the vicinity of the respective RE dopant 4d absorption thresholds. For the RE dopants studied, resonance results from a signal overlap between direct emission of photoelectrons from the 4f state

$$4d^{10}4f^N + h\nu \rightarrow 4d^{10}4f^{N-1} + e^- \qquad (1)$$

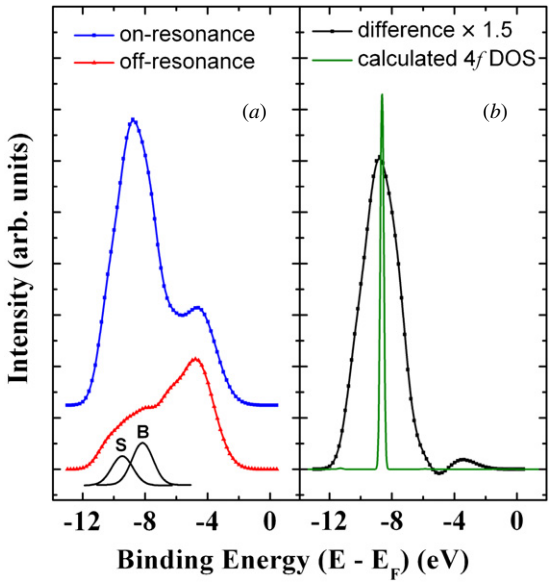

Figure 6. Energy distribution curves (*a*) of GaN:Gd for off-resonance and on-resonance photon energies of 120 and 148 eV, respectively, while more complete data sets are available in [23]. The strong, resonating surface (S) and bulk (B) Gd 4f components of the GaN:Gd valence band are illustrated. The 4f component is enhanced at the 4d absorption threshold of 148 eV, as shown in the difference spectrum, (*b*) together with the calculated 4f DOS of $Ga_{17}GdN_{18}$.

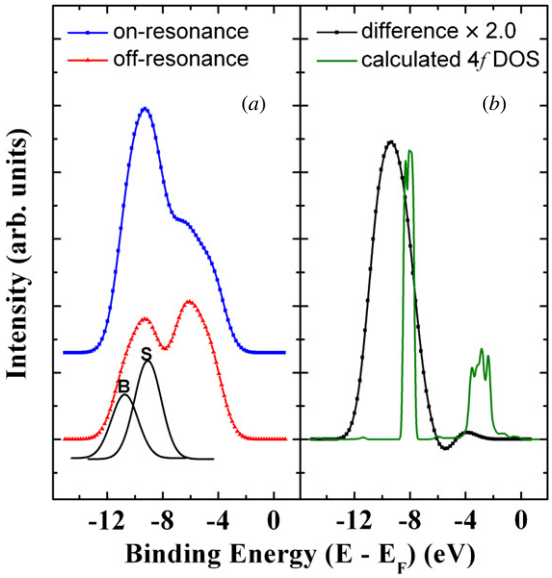

Figure 7. Energy distribution curves (*a*) of GaN:Er for off-resonance and on-resonance photon energies of 135 and 176 eV, respectively, while more complete data sets are available in [23]. The strong, resonating surface (S) and bulk (B) Er 4f components of the GaN:Er valence band are illustrated. The 4f component is enhanced at the 4d absorption threshold of 176 eV, as shown in the difference spectrum, (*b*) together with the calculated 4f DOS of $Ga_{17}ErN_{18}$.

and Auger-like electrons emitted in a super Coster–Kronig process [52]

$$4d^{10}4f^{N} + h\nu \rightarrow [4d^{9}4f^{N+1}]^{*} \rightarrow 4d^{10}4f^{N-1} + e^{-}, \qquad (2)$$

where $[]^{*}$ denotes an excited state. The final states for both the direct and recombination processes are identical.

The effects of band hybridization and dopant-induced strain between the various RE dopants and the GaN surfaces is not identical, but the valence band photoemission spectra for Er- and Gd-doped GaN are very similar as seen in figures 6 and 7, while for Yb-doped GaN, the valence band is significantly broader extending from −2 eV to nearly −14 eV. The spectra do change with photon energy and significant enhancements of some of the valence band features are seen at some photon energies [23].

For Gd-doped GaN (GaN:Gd), figure 6 shows that the intensity of the spectral features with binding energies near 8–9 eV below the Fermi level increase significantly at a photon energy of ∼148 eV. These intensity resonances for GaN:Gd [23] are very similar to those observed for Gd_2O_3 [48] and Gd-doped HfO_2 [48, 53]. This agreement further supports the assertion that the GaN:Gd spectral features at the bottom of the valence band, in the region of −9 to −10 eV in figure 6, are of strong Gd 4f weight or represent bands that strongly hybridize with the RE. Not only are the resonant photon energies similar, but also the features at the bottom of the valence band contain a strong feature at about −8 eV binding energy and a weaker shoulder in the vicinity of −10 eV binding energy. This suggests a surface and a bulk component for the Gd in GaN, in spite of the low Gd concentrations. By taking selected difference spectra for on- versus off-resonance (figure 6(*b*)), the 4f weighted DOS may be emphasized. This

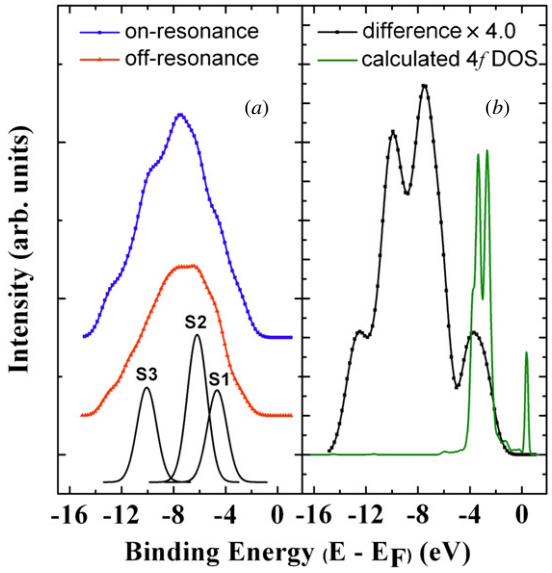

Figure 8. Energy distribution curves (*a*) of GaN:Yb for off-resonance and on-resonance photon energies of 153 and 191 eV, respectively, while more complete data sets are available in [23]. The strong, resonating surface Yb 4f components of the GaN:Yb valence band are illustrated. The 4f components are enhanced at the 4d absorption threshold of 191 eV, as shown in the difference spectrum, (*b*) together with the calculated 4f DOS of $Ga_{17}YbN_{18}$.

latter photoemission evidence supports the placement of the Gd 4f states well below the bottom of the GaN valence band, in good agreement with our expectations from theory (figure 3), in which we observe that the 4f levels are located away from majority of the host valence bands, as seen in figure 6(*b*). The negative values for the experimental 4f DOSs derived from the difference spectra are a common

artifact of obtaining the difference between photoemission spectra at one photon energy and another, as there are matrix element effect and changing cross-section of the other valence band photoemission features with photon energy. In spite of the deficiencies of taking difference spectra to extract experimental Gd 4f weight, there is general agreement with expectations (figure 6(*b*)).

Similarly, for GaN:Er, the valence band features, again at the bottom of the valence band at binding energies of roughly −8.9, and −10.7 eV, strongly resonate at photon energies of 166 and 173 eV [23]. Figure 7 shows a similar, albeit not identical, response for GaN:Er compared to GaN:Gd at the photon energy characteristic for the Er 4d → 4f super Coster–Kronig resonance at a photon energy of 176 eV. As with the GaN:Gd thin film, the spectral feature at an approximate binding energy of −9 eV in GaN:Er resonates in the range of the Er 4d absorption threshold. This is particularly clear in the difference spectra for on- versus off-resonance (figure 7(*b*)), where again the 4f weighted DOS is emphasized. Again, the negative values for the experimental 4f DOS derived from the difference spectra are a common artifact. Judging by the placement of the occupied 4f states in the photoemission spectra taken from ErAs [50], we would expect 4f contributions at both the bottom and the top of the of the valence band of GaN. The region of 4–6 eV binding energy should be dominated by the $4f_{7/2}$ (mainly the $^5I_8$ and $^5I_7$ multiplet components [50, 54, 55]), while the bottom of the valence band should be dominated by the $4f_{5/2}$ (mainly the $^3M_{10}$ and $^3L_9$ multiplet components [50, 54, 55], although there are many others). In fact, this expectation is also born out by our density function theory model calculations (figure 4) which show some of the 4f levels mixed with the valence and conduction bands, yet there are some that reside below the valence bands. The answer for why, in fact, this is not observed in the photoemission, no doubt, partly lies in the fact that there is strong hybridization of some of the 4f components with the N 2p and Ga 4p bands, as observed for ErAs [50]. In fact, the 4f placement in experiment at greater binding energies than expected from theory (figure 7(*b*)) also suggests that this system may have higher 4f correlation energies than we would otherwise anticipate, and perhaps closer to the value of 8.6 eV used previously with ErAs [50], as noted above.

Although much weaker than the resonant enhancements observed for GaN:Gd (figure 6) and GaN:Er (figure 7), there is a resonant enhancement in the valence band for GaN:Yb, particularly in the region of −6 to −7 eV binding energy, as plotted in figure 8. Figure 8 (GaN:Yb) illustrates that the intensity of photoemission features at binding energies of ∼3, ∼7 and ∼10 eV increase slightly at photon energies corresponding to the Yb 4d core in the vicinity of 191 eV. Although Yb metal should have an electronic configuration of $4d^{10}4f^{14}$, such that an exited 4d electron has no unfilled 4f state to occupy, partial 4f occupancy is still possible. Previous experimental results [56, 57], using the oxidation-induced valence change for Yb ($4f^{14}$–$4f^{13}$), determined that the data for Yb_2O_3 were well described by Fano's theory of interaction between discrete and continuum states. The depletion of the 4f occupancy appears to be related to a strong hybridization with the GaN lattice as seen in the band structure calculations for $Ga_{17}YbN_{18}$, as well as in the 4f partial DOS (figure 5(*b*)) obtained from the difference spectra for on- versus off-resonance (figure 8(*b*)), where again the 4f weighted DOS is emphasized. As seen in the band structure calculations for $Ga_{17}YbN_{18}$, as well as in the 4f partial DOS (figure 5(*b*)): almost all the 4f levels hybridize with the host valence bands, and only a few appear in the band gap. This depletion of Yb 4f filling, from $4f^{14}$ due to strong hybridization with the host GaN, results in the weak photoemission resonance in the expected location of the Yb 4f multiplets [23]. These weak photoemission resonance effects are consistent with our expectations of strong Yb hybridization with the host lattice. The Yb 4f placement within the GaN valence band does differ from what is expected, but multiconfigurational final states and shake up features are possible in photoemission and would not be apparent in a ground state calculation. There is also the possibility that we have hugely underestimated the Yb 4f correlation energies needed, and although the choice of correlation energies seems reasonable, this possibility cannot be completely excluded, in spite of a choice of a $U = 0$ eV chosen for YbAuMg [47]. A choice of a larger correlation energy would have also improved agreement between experiment and theory for GaN: Er and GaN: Gd, as noted above.

5. Summary

We find that the occupied rare earth 4f states are seen to be detached from the bottom of the GaN valence band during Gd doping. Yet some of the Er 4f levels mingle with the valence and conduction bands of the host GaN, and few 4f levels remain still located below the valence bands. Only when doped with Yb, we note nearly all the 4f levels hybridize with the GaN valance bands and a few show up in the band gap, which leads to some depletion of the $4f^{14}$ occupancy. Overall we interpret the rare earth 4f state placement based on the combined results of the photoemission and electronic structure calculations as contributing to the f–f transition spectral broadening would take place in Er- and Yb-doped GaN due to the strong hybridization of the GaN matrix with the imbedded rare earth 4f states.

Acknowledgments

This work was supported by the Defense Threat Reduction Agency (DTRA) through grant nos HDTRA1-07-1-0008 and BRBAA08-I-2-0128, the Nebraska Materials Science and Engineering Center (DMR-0820521), the Institute for Functional Nanomaterials and NASA-IDEA-PR. This work was supported by Nebraska Research Initiative and DOE DE-EE0003174. The University of Nebraska Holland Computing Center provided the computational resources with the associated USCMS Tier-2 site at the University of Nebraska–Lincoln. The views expressed in this paper are those of the authors and do not reflect the official policy or position of the Air Force, Department of Defense, or the US Government.

References

[1] Koubaa T, Dammak K, Kammoun M, Jadwisienczak W M and Lozykowski H J 2010 *J. Alloys Compd.* **496** 56–60
[2] Koubaa T, Dammak M, Kammoun M, Jadwisienczak W M, Lozykowski H J and Anders A 2009 *J Appl. Physiol.* **106** 013106
[3] Jadwisienczak W M and Lozykowski H J 2003 *Opt. Mater.* **23** 175
[4] Kenyon A J 2002 *Prog. Quantum Electron.* **26** 225
[5] Park J H and Steckl A J 2008 *Phys. Status Solidi* a **205** 26
[6] Nishikawa A, Kawasaki T, Furukawa N, Terai Y and Fujiwara Y 2009 *Appl. Phys. Express* **2** 1004
[7] Steckl A J, Heikenfeld J, Lee D S and Garter M 2001 *Mater. Sci. Eng.* B **81** 97–101
[8] Tao J H, Perea-Lopez N, McKittrick J, Talbot J B, Klinedinst K, Raukas M, Laski J, Mishra K C and Hirata G 2008 *Phys. Status Solidi* c **5** 1889
[9] Shi J, Chandrashekhar M V S, Reiherzer J, Schaff W, Lu J, Disalvo F and Spencer M G 2008 *Phys. Status Solidi* c **5** 1495
[10] Jadwisienczak W, Wisniewski K, Spencer M, Thomas T and Ingram D. 2010 *Radiat. Meas.* **45** 500–2
[11] Okada H, Nakanishi Y, Wakahara A, Yoshida A and Ohshima T 2008 *Nucl. Instrum. Methods Phys. Res.* B **266** 853–6
[12] Nakanishi Y, Wakahara A, Okada H, Yoshida A, Ohshima T and Itoh H 2002 *Appl. Phys. Lett.* **81** 1943–5
[13] Thomas T *et al* 2009 *J. Cryst. Growth* **311** 4402–7
[14] Steckl A J, Park J H and Zavada J M 2007 *Mater. Today* **10** 20–27
[15] Dieke G H and Crosswhite H M 1963 *Appl. Opt.* **2** 675–86
[16] Gschneidner K A and Eyring L R 1978 *Handbook on The Physics and Chemistry of Rare Earths* vol 1 (Amsterdam: North-Holland) p 88
[17] Lozykowski H J, Jadwisienczak W M and Brown I 2000 *J. Appl. Phys.* **88** 210
[18] Andreev T, Liem N Q, Hori Y, Tanaka M, Oda O, Dang D L S and Daudin B 2006 *Phys. Rev.* B **73** 195203
[19] Filhol J-S, Jones R, Shaw M J and Briddon P R 2004 *Appl. Phys. Lett.* **84** 2841
[20] Hourahine B, Sanna S, Aradi B, Köhler C and Frauenheim T 2006 *Physica* B **376** 512
[21] Svane A, Christensen N E, Petit L, Szotek Z and Temmerman W M 2006 *Phys. Rev.* B **74** 165204
[22] Jones R and Hourahine B 2010 *Rare Earth Doped III-Nitrides For Optoelectronic And Spintronic Applications Topics in Applied Physics* vol 124 (Berlin: Springer) pp 1–24
[23] McHale S R, McClory J W, Petrosky J C, Wu J, Palai R, Losovyj Y B and Dowben P A 2011 *Eur. Phys. J.: Appl. Phys.* **56** 11301
[24] Plucinski L *et al* 2005 *Solid State Commun.* **136** 191
[25] Chiang T C and Eastman D E 1980 *Phys. Rev.* B **21** 5749
[26] Suzuki S, Kiyokura T, Maeda F, Nath K G, Watanabe Y, Saitoh T and Kakizaki A 2001 *J. Electron Spectrosc.* **114** 421
[27] Maruyama T, Morishima S, Bang H, Akimoto K and Nanishi Y 2002 *J. Cryst. Growth* **237** 1167
[28] Ketsman I, Losovyj Y B, Sokolov A, Tang J, Wang Z, Belashchenko K D and Dowben P A 2007 *Appl. Phys.* A **89** 489–92
[29] Sabirianov R F, Mei W N, Lu J, Gao Y, Zeng X C, Bolskar R D, Jeppson P, Wu N, Caruso A N and Dowben P A 2007 *J. Phys.: Condens. Matter* **19** 082201
[30] Ketsman I, Losovyj Y B, Sokolov A, Tang J, Wang Z, Natta M, Brand J I and Dowben P A 2008 *Appl. Surf. Sci.* **254** 4308–12
[31] McHale S R, McClory J W, Petrosky J C, Wu J, Rivera A, Palai R, Losovyj Y B and Dowben P A 2011 *Eur. Phys. J.: Appl. Phys.* **55** 31301
[32] McHale S R, McClory J W, Petrosky J C, Wu J, Palai R, Dowben P A and Ketsman I 2011 *Mater. Lett.* **65** 1476
[33] Losovyj Y, Ketsman I, Morikawa E, Wang Z, Tang J and Dowben P A 2007 *Nucl. Instrum. Methods Phys. Res.* A **582** 264
[34] Hormes J, Scott J D and Suller V P 2006 *Synchrotron Radiat. News* **19** 27
[35] Roy A, Morikawa E, Bellamy H, Kumar C, Goettert J, Suller V, Morris K, Ederer D and Scott J 2007 *Nucl. Instrum. Methods Phys. Res.* A **582** 22–5
[36] Morikawa E, Scott J D, Goettert J, Aigeldinger G, Kumar C S S R, Craft B C, Sprunger P T, Tittsworth R C and Hormes F J 2002 *Rev. Sci. Instrum.* **73** 1680–3
[37] Dowben P A, LaGraffe D and Onellion M 1989 *J. Phys.: Condens. Matter* **1** 6571
[38] Segall M D, Philip J D L, Probert M J, Pickard C J, Hasnip P J, Clark S J and Payne M C 2002 *J. Phys.: Condens. Matter* **14** 2717
[39] Perdew J P, Burke K and Ernzerhof M 1996 *Phys. Rev. Lett.* **77** 3865
[40] Marzari N, Vanderbilt D and Payne M C 1997 *Phys. Rev. Lett.* **79** 1337
[41] Payne M C, Teter M P, Allan D C, Arias T A and Joannopoulos J D 1992 *Rev. Mod. Phys.* **64** 1045
[42] Sabiryanov R F and Jaswal S S 1997 *Phys. Rev.* B **55** 4117
[43] Harmon B N, Antropov V P, Liechtenstein A I, Solovyev I V and Anisimov V I 1995 *J. Phys. Chem. Solids* **56** 1521
[44] Duan C G, Sabiryanov R F, Liu J J, Mei W N, Dowben P A and Hardy J R 2005 *Phys. Rev. Lett.* **94** 237201
[45] Duan C G, Sabiryanov R F, Mei W N, Dowben P A, Jaswal S S and Tsymbal E Y 2007 *J. Phys.: Condens. Matter* **19** 315220
[46] Lu J, Sabirianov R F, Mei W N, Gao Y, Duan C G and Zeng X C 2006 *J. Phys. Chem.* B **110** 23637
[47] Gegner J, Koethe T C, Wu H, Hu Z, Hartmann H, Lorenz T, Fickenscher T, Pöttgen R and Tjeng L H 2006 *Phys. Rev.* B **74** 073102
[48] Losovyj Y B *et al* 2009 *J. Phys.: Condens. Matter* **21** 045602
[49] Sabirianov R F, Mei W N, Lu J, Gao Y, Zeng X C, Bolskar R D, Jeppson P, Wu N, Caruso A N and Dowben P A 2007 *J. Phys.: Condes. Matter* **19** 082201
[50] Komesu T, Jeong H-K, Choi J, Borca C N, Dowben P A, Petukhov A G, Schultz B D and Palmstrøm C J 2003 *Phys. Rev.* B **67** 035104
[51] Monkhorst H J and Pack J D 1976 *Phys. Rev.* B **13** 5188
[52] Wendin G 1981 *Breakdown of One Electron Pictures in Photoelectron Spectra Structure and Bonding* vol 45 (Berlin: Springer)
[53] Ketsman I, Losovyj Y B, Sokolov A, Tang J, Wang Z, Belashchenko K D and Dowben P A 2007 *Appl. Phys.* A **89** 489
[54] Lang J K, Baer Y and Cox P A 1981 *J. Phys. F* **11** 121
[55] Stauffer L, Pirri C, Wetzel P, Mharchi A, Paki P, Bolmont D, Gewinner G and Minot C 1992 *Phys. Rev.* B **46** 13201
[56] Schmidt-May J, Gerken F, Nyholm R and Davis L C 1984 *Phys. Rev.* B **30** 5560
[57] Sun Y M and Wu M C 1995 *J. Appl. Phys.* **78** 6691